Low-dimensional ferroelectrics under different electrical and mechanical boundary conditions: Atomistic simulations

I. Ponomareva,* I. I. Naumov,† and L. Bellaiche‡
Department of Physics, University of Arkansas, Fayetteville, Arkansas 72701, USA
(Received 7 September 2005; published 21 December 2005)

Ferroelectric nanodots and infinite wires of $Pb(Zr_{0.4}Ti_{0.6})O_3$ alloy under different boundary conditions are investigated via Monte Carlo simulations using an atomistic first-principles-based effective Hamiltonian. These nanosystems all exhibit a spontaneous polarization that points along a nonperiodic direction, for situations close to short-circuit electrical boundary conditions and independently of the epitaxial strain. On the other hand, unusual dipole patterns arise in these systems when they are under open-like circuit conditions. The dependency of these patterns on the nanostructure's dimensionality and strain is further revealed and explained.

DOI: 10.1103/PhysRevB.72.214118 PACS number(s): 77.22.Ej, 77.80.Bh, 77.84.Dy

I. INTRODUCTION

Intense effort has been recently made in synthesizing, characterizing, and/or simulating ferroelectric nanostructures (FENs) because of their technological and fundamental promise (see, e.g., Refs. 1–17 and references therein). Among the different possible classes of FENs, the [two-dimensional-like (2D-like)] thin films are, by far, the ones that have been the most investigated. As a result, their properties begin to be rather well determined and understood. On the other hand, studies on zero-dimensional-like (0D-like) and one-dimensional-like (1D-like) FENs are rather scarce, despite their potential in resulting to interesting phenomena. For instance, Refs. 8 and 9 predicted that nanodots, nanodisks, and nanorods all exhibit a vortex structure for their electrical dipoles—leading to a nonzero toroid moment of polarization rather than a net polarization—when under specific boundary conditions, namely, stress-free and open circuit. In our minds, what is crucially missing nowadays is to know and understand how properties of 0D-like and 1D-like FEN depend on mechanical and electrical boundary conditions—which is a feature solely known in ferroelectric thin films.[7,12,11] As a matter of fact, such boundary conditions most likely have a dramatic effect on the FENs properties and can vary from one experimental setup to another, depending (i) on the used substrate, (ii) if the FENs are embedded in a insulating versus metallic host, or (iii) if the FENs are placed in a reactive atmosphere able to modify the FENs surfaces composition.

The main aim of this paper is to fill up this gap by investigating ferroelectric nanodots and nanowires under different electrical and mechanical boundary conditions. Our systematic study not only reveals unusual striking dipole patterns of these ferroelectric nanostructures, but also allows one to understand how and why the different classes of low-dimensional ferroelectrics (e.g., dots, wires, films) can differ or look alike when under similar boundary conditions.

II. METHODOLOGY

We decided to focus on dots and wires made of (disordered) $Pb(Zr_{0.4}Ti_{0.6})O_3$ solid solutions for mostly two reasons. First of all, such alloys are technologically important. Second, our chosen Ti composition allows us to explore how mechanical and electrical boundary conditions should, typically (e.g., as in the $PbTiO_3$ simple system), affect electrical dipoles in low-dimensional ferroelectrics. In other words, we purposely avoid investigating lead-zirconate-titanate (PZT) alloys with smaller Ti concentration because (i) anomalous features (such as the easiness of rotating the spontaneous polarization) occur in PZT bulks for Ti content ranging between $\simeq$46 and $\simeq$51 %,[18] and (ii) the rather unusual antiferrodistortive rotation of the oxygen octahedra can be activated, and compete with ferroelectricity, in $Pb(Zr_{1-x}Ti_x)O_3$ bulks with x smaller than $\simeq$50%.[19]

In this paper, the x-, y- and z-axes are chosen along the pseudocubic [100], [010], and [001] directions, respectively. The nanostructures are represented by supercells that are either finite in any direction, in the case of dots, or repeated periodically *along the z direction*, in the case of nanowires. We typically use supercells of 48 Å length (12 unit cells) in any nonperiodic direction. Moreover, two different supercells of 12 and 24 unit cells, respectively, along the z-periodic direction have been chosen to mimic the (same) infinite wire, in order to check the dependency of its properties on the supercell choice. The total energy of such supercells is written as

$$\mathcal{E}_{Heff}(\mathbf{p_i}, \mathbf{v_i}, \eta, \sigma_i) + \beta \sum_i \langle \mathbf{E}_{dep} \rangle \mathbf{p_i} \quad (1)$$

where $\mathbf{p_i}$ is the local dipole at site i of the supercell and $\mathbf{v_i}$ are inhomogeneous-strain-related variables around this site i. η is the homogeneous strain tensor while σ_i represents the atomic configuration of the alloy.[20] The expression and first-principles-derived parameters of (the alloy effective Hamiltonian) $\mathcal{E}_{Heff}$ energy are those given in Ref. 20 for PZT *bulk*, except for the dipole-dipole interactions for which we use the analytical expressions derived in Ref. 21 for nanostructures *under ideal open-circuit (OC) conditions*. Such dipole-dipole interactions depend on the dimensionality of the system; that is, their expressions differ for the case of dots (that are finite along any Cartesian direction) and wires (that are infinitely periodic along a single Cartesian direction). The second term

of Eq. (1) mimics a screening of the maximum (i.e., associated with ideal OC conditions and dipoles having non-null Cartesian components along nonperiodic directions) depolarizing field $\langle \mathbf{E}_{dep} \rangle$ inside the FEN, with the magnitude of this screening being controlled by the β coefficient. $\beta=1$ and $\beta=0$ corresponds to ideal short circuit (SC) (full screening of $\langle \mathbf{E}_{dep} \rangle$) and OC (no screening of $\langle \mathbf{E}_{dep} \rangle$) electrical boundary conditions, respectively. A value of β in between corresponds to more realistic electrical boundary situation for which a residual depolarizing field exists inside the nanostructure.[12] Technically, $\langle \mathbf{E}_{dep} \rangle$ is calculated at an atomistic level via the recently proposed approach of Ref. 22, and (naturally) depends on the dimensionality, size, and dipoles pattern of the investigated nanostructure. Note that decomposing the total energy of nanostructures under a residual depolarizing field as a sum of one term depending on bulk parameters and a second term associated with the internal field, as done in Eq. (1), has been shown[11,12] to reproduce very well direct first-principles[12] and experimental results.[7] We will simulate different electrical boundary conditions by changing the value of the screening coefficient β (or equivalently, the magnitude of the residual depolarizing field).

Different mechanical boundary conditions can also be simulated[11,14] thanks to the homogeneous strain η. For example, during the simulation associated with a substrate-induced strain in the (x,z) plane, three components of η—in voigt notation—are kept fixed (namely, $\eta_5=0$, and $\eta_1=\eta_3=\delta$, with δ characterizing the lattice mismatch between PZT and a chosen substrate), while the other three components relax.[27] On the other hand, *all* the components of strain tensor are allowed to relax during the simulation of freestanding (i.e., stress-free) system.

The energy of Eq. (1) is used in Monte Carlo (MC) simulation to determine the ground state of the investigated FEN. Practically, we use the following procedure to, indeed, determine the ground-state rather than a local minimum: every simulation starts from a high temperature $T=2000$ K, and is then followed by a two-step annealing. The annealing rates for the first ($100\ \mathrm{K} < T < 2000\ \mathrm{K}$) and second ($10\ \mathrm{K} < T \leqslant 100\ \mathrm{K}$) steps are 100 K/40 000 MC sweeps and 10 K/40 000 MC sweeps, respectively. Finally, the simulation runs for 40 000 MC sweeps at $T=10$ K, which provides us with an accurate measure of the ground-state configuration.

III. RESULTS

We first investigate how electrical boundary conditions affect structural properties of a *freestanding* cubic finite nanodots of 48 Å lateral size and of a *stress-free* nanowire that is periodic along the z direction (chosen along the pseudocubic [001] direction) and that has a cubic cross section of 48×48 Å^2. The results of our simulation for the spontaneous polarization are shown in Figs. 1(a) and 1(c) for the dot and wire, respectively. The left and right insets of Figs. 1(a) and 1(c) further display a cross section of a snapshot of the dipole pattern for ideal OC and SC conditions, respectively, in these two systems. Under perfect SC conditions ($\beta=1$), the dot and nanowire exhibit a spontaneous polarization having a

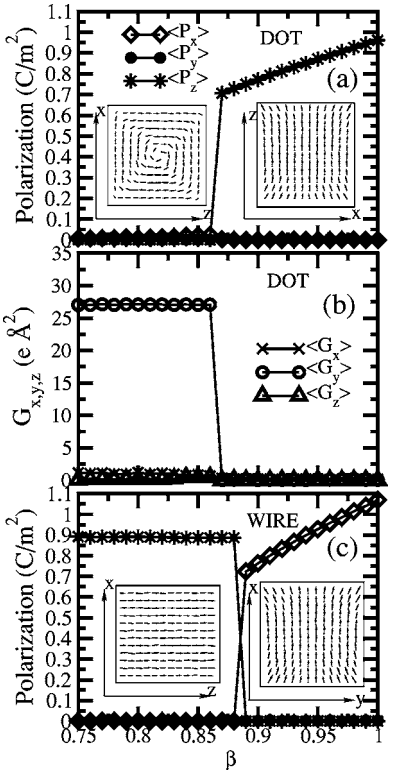

FIG. 1. Ground-state spontaneous polarization in freestanding dot (a) and wire (c) as a function of the screening coefficient β. The β dependency of the toroid moment of polarization in the freestanding nanodot is shown in (b). Right and left insets to both (a) and (b) show the projection of the dipole patterns on a chosen plane for perfect SC and OC conditions, respectively, in the corresponding nanostructure. (Note that these dipoles nearly lie in the plane shown in the insets; that is, there is only a slight difference between the dipole vectors and their displayed projections.) The infinite direction of the wire is along the z-axis. The x-, y-, and z-axes are chosen along the pseudocubic [100], [010], and [001] directions, respectively.

magnitude 0.96 and 1.07 C/m^2, respectively, that is rather close to that of the corresponding bulk material (1.00 C/m^2) calculated within the alloy effective Hamiltonian technique.[28] The resulting dipole patterns are very similar in the two low-dimensional ferroelectrics, with the exception that the dipoles can point along any $\langle 100 \rangle$ pseudocubic direction (i.e., along the x-or y- or z-axis) in the dot, while they can only align along the x- or y-axis in the wire; that is, they align along a $\langle 100 \rangle$ direction that is *perpendicular* to the infinite (z) direction of the wire. The desire of nanostructures under SC to have a spontaneous polarization lying along a *finite* direction has been previously found in ferroelectric thin films[11,13] and is mostly caused by a gain in energy related to short-range effects.[13]

Decreasing the β parameter with respect to the one associated with perfect short-circuit electrical boundary conditions induces a residual depolarizing field, whose magnitude is proportional to $1-\beta$. Such field opposes—and thus wants to suppress—the spontaneous polarization. This is clearly indicated by the linear decrease of the polarization magnitude seen in Figs. 1(a) and 1(c) when decreasing β from 1 to some

critical value around 0.88, corresponding to a 88 % screening of the maximum depolarizing field, in both the nanodot and the wire.

Below these critical values, the magnitude of the residual depolarizing field inside the FEN becomes so large than the dipoles have to rearrange themselves to efficiently suppress it. A structural phase transition thus occurs. In case of the dot, such transition is characterized by the vanishing of the spontaneous polarization (as also found in Ref. 23 for some $BaTiO_3$ nanodots under open-circuit conditions), and the formation of a vortex dipole structure [see left inset of Fig. 1(a)] that results in the appearance of a spontaneous toroid moment of polarization,[9] as indicated by Fig. 1(b). Interestingly, the wire energetically chooses a different dipole pattern [see left inset of Fig. 1(c)] to annihilate the macroscopic depolarization field, namely, the dipoles now align along the infinite direction of this wire (rather than perpendicular to it as for SC conditions). This difference between the dipole pattern in the dot versus the wire can be simply understood by realizing that, unlike the wire, the dot is confined along *any* direction. As a result, any nonzero macroscopic polarization pointing along any direction would lead to the activation of a depolarizing field in the dot. Moreover, the infinite wire prefers to have a macroscopic polarization rather than adopting a vortexlike dipole pattern below a critical value of β because the formation of such latter pattern is more costly in terms of short-range and elastic energies. Similarly, stress-free thin films under OC-like conditions have also been found to have a macroscopic polarization pointing along a periodic direction.[11] Interestingly, Figs. 1(b) and 1(c) and Ref. 11 tell us that the magnitude of the order parameter—that is, the spontaneous polarization in wires and films *versus* spontaneous toroid moment of polarization in the dot—in stress-free FENs is independent of β below the critical values. In other words, a given FEN adopts a *specific* dipole pattern to fight once and for all against the depolarizing field, once this field is large enough.

We next turn our attention to the same dot and wire, but under different mechanical boundary conditions, namely, those mimicking an epitaxial growth in the (x,z) planes. The infinite (z) direction of the wire is thus chosen to lie in such planes. The results for a *tensile* strain δ of +2.65 % are shown in Fig. 2 and are overall qualitatively close to the corresponding ones in the freestanding systems. There are, however, three differences worth of attention. First of all, dipoles aligned along the z- or x-axis are now preferred over dipoles parallel to the y-axis because of our chosen tensile strains. This implies that the spontaneous polarization of the dot under electrical boundary conditions close to SC can only be along the x- or z-axis, i.e, it now has to avoid the y-axis. Similarly, the wire under SC and tensile strain exhibits a macroscopic polarization that is solely aligned along the x-axis, whereas for stress-free mechanical conditions, such polarization had an equal probability to be parallel to either the x- or y-axis. These tensile strains also imply that the toroid moment of the dot under OC-like conditions can only be along the y-axis as opposed to the case of stress-free dots for which this moment has an equal probability to be along any of the three Cartesian directions. Second, the magnitudes of the spontaneous polarization and toroid moment are larger

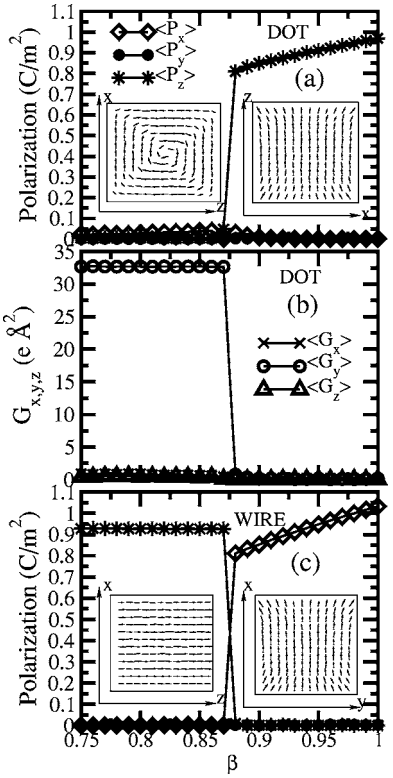

FIG. 2. Ground-state spontaneous polarization in dot (a) and wire (c), under a tensile strain +2.65 % applied in the (x,z) plane, as a function of the screening coefficient β. The β dependency of the toroid moment of polarization in the nanodot is shown in (b). Right and left insets to both (a) and (b) show the projection of the dipole patterns on a chosen plane for perfect SC and OC conditions, respectively, in the corresponding nanostructure. (Note that these dipoles nearly lie in the plane shown in the insets; that is, there is only a slight difference between the dipole vectors and their displayed projections.) The infinite direction of the wire is along the z-axis. The x-, y-, and z-axes are chosen along the pseudocubic [100], [010], and [001] directions, respectively.

than those of the freestanding systems for small β. Such a feature is due to the fact that the x- and z-components of the dipoles expand as a result of their coupling with the tensile strains.[24–26] Third, we numerically found another configuration (Fig. 3) for a nanowire under tensile strain, and with β smaller than 86 %, that is slightly larger in energy than the configuration shown in the left part of the inset of Fig. 2(c). It consists of an infinite number of vortexes assembled along the z direction of the wire, with neighboring vortexes rotating in opposite directions. The formation of this configuration is driven by the desire of the wire to have nonzero components of the dipole in *both* x and z directions, as dictated by the tensile strain, while minimizing the depolarizing field inside the wire.

We now study the effect of a *compressive* strain δ of −2.65 %—still applied in the (x,z) plane—on the dipole pattern in the nanodot and wire. The results of our simulation are shown in Fig. 4. Such compressive strain favors dipoles aligned along the y-axis via the strain-dipole coupling,[24–26] which explains why the spontaneous polarization of the dot and wire lies along such direction for electrical boundary

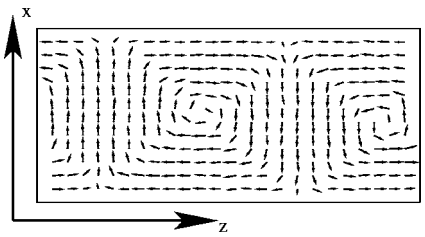

FIG. 3. A cross section of another possible dipole pattern for a nanowire periodic along the z direction, and under OC-like electrical boundary conditions and a tensile strain applied in the (x,z) plane. The arrows show the projection of the dipole patterns on a chosen plane. (Note that these dipoles nearly lie in the plane shown in the insets; that is, there is only a slight difference between the dipole vectors and their displayed projections.) The x-, y-, and z-axes are chosen along the pseudocubic [100], [010], and [001] directions, respectively.

conditions close to SC (see Figs. 4(a) and 4(c) and their right insets). However, for the smallest β values, any macroscopic polarization aligned along the y-axis would generate a relatively large depolarizing field that should strongly oppose such polarization. The resulting ground-state configurations must thus arise from a compromise between these strain *versus* depolarizing field factors. As a result, both nanosystems form 180° stripe domain with the dipoles being mostly "up" or "down" along the y direction, with two neighboring and opposite stripes having a very small overall thickness (namely, 48 Å in the present case). Interestingly, such *nanodomain* patterns occur in *any* low-dimensional ferroelectrics under compressive strain and under residual depolarizing field since they have also been found in ferroelectric thin films experiencing similar mechanical and electrical boundary conditions.[7,11] Note, however, that the wires and films distinguish themselves from the dot in the sense that the former exhibit stripe domains that are (infinitely) repeated along a periodic direction, while the three-dimensional confinement of the nanodot results in a finite number of stripes. Furthermore, unlike for the strain-free and tensile mechanical boundary conditions, the ground-state dipole pattern in the compressively strained dot leads to a vanishing spontaneous (total) toroid moment of polarization,[29] in addition to a vanishing spontaneous polarization, for small β.

IV. CONCLUSIONS

In summary, we have used a first-principles-derived scheme to reveal the rich variety of dipole patterns that can occur in ferroelectric nanodots and nanowires as a result of the interplay between mechanical and electrical boundary conditions. We also discussed, and explained, the differences and resemblances that 2D, 1D, and 0D nanostructures can have when placed under similar boundary conditions. We are thus confident that this study leads to a deeper understanding of low-dimensional ferroelectrics, in general, and will help in interpreting future experimental data, in particular.

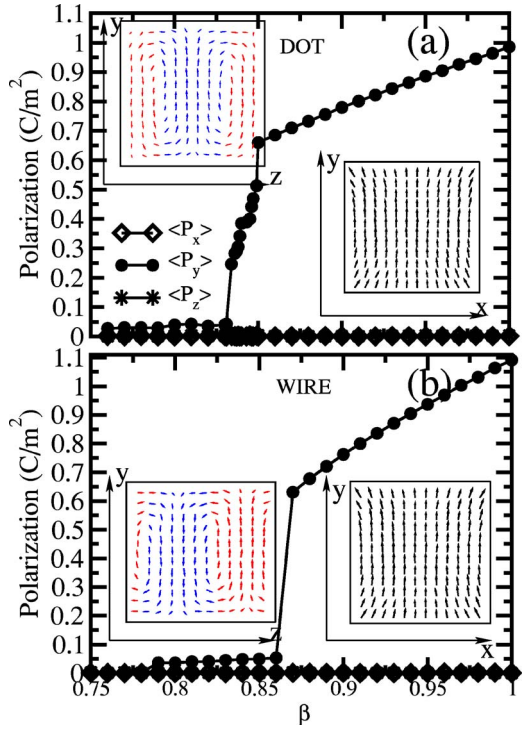

FIG. 4. (Color online). Ground-state spontaneous polarization in dot (a) and wire (b), under a compressive strain −2.65 % in the (x,z) plane, as a function of the screening coefficient β. Right and left insets to both (a) and (b) show the projection of the dipole patterns on a chosen plane for perfect SC and OC conditions, respectively, in the corresponding nanostructure. (Note that these dipoles nearly lie in the plane shown in the insets; that is, there is only a slight difference between the dipole vectors and their displayed projections.) The infinite direction of the wire is along the z-axis. The x-, y-, and z-axes are chosen along the pseudocubic [100], [010], and [001] directions, respectively.

ACKNOWLEDGMENTS

We thank I. Kornev, Huaxiang Fu, and J. Spanier for useful discussions. This work was supported by NSF Grants No. DMR-0404335 and No. DMR-9983678, by ONR Grants No. N00014-01-1-0365, No. N00014-04-1-0413, and No. N00014-01-1-0600 and by DOE Grant No. DE-FG02-05ER46188.

*Electronic address: iponoma@uark.edu
†Electronic address: inaumov@uark.edu
‡Electronic address: laurent@uark.edu

[1] I. Szafraniak and M. Alexe, Ferroelectrics **291**, 19 (2003).
[2] J. J. Urban, W. S. Yun, Q. Gu, and H. Park, J. Am. Chem. Soc. **124**, 1186 (2002).
[3] W. S. Yun, J. J. Urban, Q. Gu, and H. Park, Nano Lett. **2**, 447 (2002).

[4] J. J. Urban, J. E. Spanier, L. Ouyang, W. S. Yun, and H. Park, Adv. Mater. (Weinheim, Ger.) **15**, 425 (2003).
[5] A. A. Sirenko, I. A. Akimov, J. R. Fox, A. M. Clark, H.-C. Li, W. Si, and X. X. Xi, Phys. Rev. Lett. **82**, 4500 (1999).
[6] O. Tikhomirov, H. Jiang, and J. Levy, Phys. Rev. Lett. **89**, 147601 (2002).
[7] D. Fong, G. Stephenson, S. Streiffer, J. Eastman, O. Auciello, P. Fuoss, and C. Thompson, Science **304**, 1650 (2004).
[8] H. Fu and L. Bellaiche, Phys. Rev. Lett. **91**, 257601 (2003).
[9] I. I. Naumov, L. Bellaiche, and H. Fu, Nature (London) **432**, 737 (2004).
[10] K. Rabe and P. Ghosez, J. Electroceram. **4:2/3**, 379 (2000).
[11] I. Kornev, H. Fu, and L. Bellaiche, Phys. Rev. Lett. **93**, 196104 (2004).
[12] J. Junquera and P. Ghosez, Nature (London) **422**, 506 (2004).
[13] P. Ghosez and K. M. Rabe, Appl. Phys. Lett. **76**, 2767 (2000).
[14] N. A. Pertsev, V. G. Kukhar, H. Kohlstedt, and R. Waser, Phys. Rev. B **67**, 054107 (2003).
[15] B.-K. Lai, I. Kornev, L. Bellaiche, and G. J. Salamo, Appl. Phys. Lett. **86**, 132904 (2005).
[16] E. Almahmoud, Y. Navtsenya, I. Kornev, H. Fu, and L. Bellaiche, Phys. Rev. B **70**, 220102(R) (2004).
[17] G. Geneste, E. Bousquet, J. Junquera, and P. Ghosez, cond-mat/0503362, Appl. Phys. Lett. (to be published).
[18] B. Noheda, D. E. Cox, G. Shirane, R. Guo, B. Jones, and L. E. Cross, Phys. Rev. B **63**, 014103 (2001).
[19] R. Ranjan, Ragini, S. K. Mishra, D. Pandey, and B. Kennedy, Phys. Rev. B **65**, 060102(R) (2002).
[20] L. Bellaiche, A. Garcia, and D. Vanderbilt, Phys. Rev. Lett. **84**, 5427 (2000); Ferroelectrics **266**, 41 (2002).
[21] I. Naumov and H. Fu, cond-mat/0505497 (unpublished).
[22] I. Ponomareva, I. Naumov, I. Kornev, H. Fu, and L. Bellaiche, Phys. Rev. B **72**, 140102(R) (2005).
[23] M. G. Stachiotti, Appl. Phys. Lett. **84**, 251 (2004).
[24] W. Zhong, D. Vanderbilt, and K. M. Rabe, Phys. Rev. B **52**, 6301 (1995).
[25] W. Zhong, D. Vanderbilt, and K. M. Rabe, Phys. Rev. Lett. **73**, 1861 (1994).
[26] R. E. Cohen, Nature (London) **358**, 136 (1992).
[27] The assumption of homogeneously strained nanodots and nanowires should be realistic for the ultrasmall nanostructures we considered here. On the other hand, the strain may become inhomogeneous and significantly relax near the upper surface for thicker systems (which are not the focus of this paper). Our study, nevertheless, provides a good starting point for the understanding of thicker nanostructures and also allows a comprehensive comparison of intrinsic properties between dots, wires, and films.
[28] Note that experimental values of spontaneous polarization may be smaller than theoretical ones because of extrinsic problems, such as defects and sample quality. In particular, grown PZT compounds are ceramics rather than single crystals.
[29] Note that the total toroid moment of polarization is an ill-defined quantity in any periodic *infinite* system (such as wires) because its value would depend on the relative position of the dipole pattern within the periodic supercell.